INTERFACE RECONSTRUCTION WITH MAGNETIC FIELD TOMOGRAPHY SYSTEM

Marek Ziolkowski[1,2], Hartmut Brauer[1], Milko Kuilekov[1],
[1]*Technische Universitaet Ilmenau,* [2]*Technical University of Szczecin, marek.ziolkowski@tu-ilmenau.de*
Invited Paper

Abstract – *There are several applications in magnetic fluid dynamics where it is important to know the behaviour of internal fluid surfaces. Magnetic field tomography enables to reconstruct the interface shape between two conducting fluids on the basis of magnetic field measurements. We describe a magnetic field tomography system for the identification and reconstruction of the interface in a cylindrical two-fluid system containing a liquid metal. The reconstruction is performed with a help of stochastic optimization techniques (genetic algorithms, simulated annealing).*

1. INTRODUCTION

In magnetic fluid dynamics (MFD) several applications of material processing, metal melting or aluminium electrolysis require deep knowledge of the behaviour of the surface of liquid metals. In the case of aluminium melting in a reduction cell we are interested in how the strong current flow acts on the motion of the surface of the molten aluminium. Because the motion can cause undesired high deformation of the surface it is important to have an opportunity to detect this deformation [1, 2]. Due to the limited access (high temperature, corrosive chemistry), the use of probes, though necessary for an appropriate control, is difficult or almost impossible. This is the reason why it is important to develop appropriate diagnostic methods for such cells.

We have recently developed a magnetic field tomography (MFT) system which enables us to reconstruct the interface between two conducting fluids using magnetic field measurements taken in a set of positions close to the surface of the object [3]. In the paper we present some results received with the help of this system related to the simulated data.

2. HIGHLY SIMPLIFIED ALUMINIUM CELL MODEL

If we consider typical figures of aluminum electrolysis cells it must be noticed that the cross section has a length of about $L = 8$ m, whereas the interface displacement η is very small compared to the lateral extent of the system. Consequently, our physical model is characterized by a very small ratio η/L.

The considered problem is shown in Fig. 1. Two fluids with different electrical conductivities σ_1 (*up*) and σ_2 (*down*), are situated in a long cylinder with the radius R. The cylinder walls are non-conducting. Along the length axis of the cylinder a homogeneous electrical current density $\mathbf{J_0}$ is applied.

If the interface between fluids is flat, the current density **J** is homogeneous everywhere. As soon as the interface deviates from its flat shape due to interfacial waves or an external forcing, the current density **J** will become inhomogeneous near the interface (Fig. 2). The inhomogeneity of **J** can be represented by the perturbation current density **j**. If the perturbation of the fluid interface is non-axisymmetric, it leads to a perturbation of the radial and axial component of the magnetic field outside the cylinder

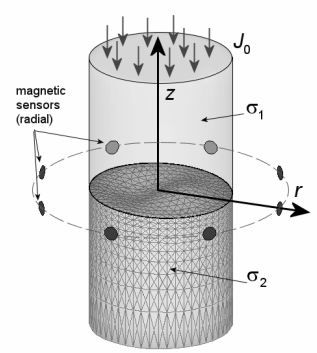

Fig. 1. *Simplified model of the cylindrical two-fluid cell.*

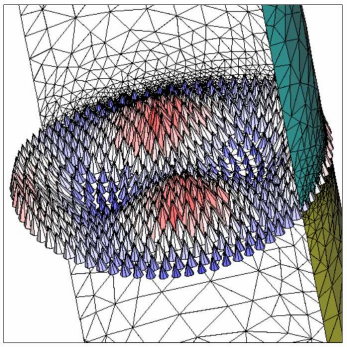

Fig. 2. *Current density distribution in the vicinity of the interface.*

The complete interface perturbation can be described by solving the Euler equation and the mass conservation law as

$$\eta(r,\alpha) = A\sum_{m=-M}^{M}\sum_{n=1}^{N}\eta_{mn}^{*}J_m(k_{mn}r)\cos(m\alpha), \qquad (1)$$

where A denotes an amplitude of the interface, η^*_{mn} are normalized mode coefficients, and J_m are Bessel functions. The value n is called the *radial* mode number and the value m the *azimuthal* mode number. Although the quantity of modes is unlimited, usually the highest modes have the smallest amplitudes and therefore can be neglected in the analysis.

3. INTERFACE RECONSTRUCTION SYSTEM

In our analysis we assume that the oscillating interface has been found in a steady state, i.e. for a certain time period the components of the interface shape are the same and only the amplitude A varies in time. Because the frequency of

oscillations is small we can apply the following procedure. We record the sensor signals for a defined time and then we look for the time moment in which the signal reaches the maximum. That time moment corresponds to the maximum of the interface amplitude and the further analysis can be performed as a static one. The sample configuration of the sensors is shown in Fig. 3 [5].

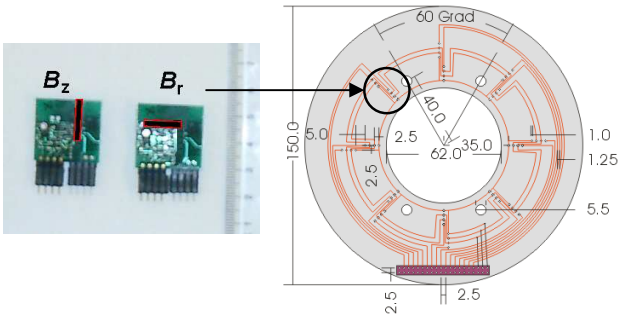

Fig. 3. *2D magnetic sensor and the scheme of sensor ring.*

The inverse problem of the magnetic field tomography is formulated as follows: having the magnetic field flux density distribution (b_r, b_z components) in the sensors positions around the cylinder we would like to reconstruct the interface shape described by (1).

The reconstruction of the interface consists in finding the amplitude A and all coefficients η^*_{mn} (1). We define two principal reconstruction tasks, first we would like to find the dominant mode in the interface η^d_{mn} and its amplitude A^d. This task we call PCA, a principal component analysis. In the second one, called a full mode task, we look for the interface amplitude A and all coefficients η^*_{mn} for given values of M and N.

The identification procedures are based on various stochastic searching techniques such as genetic algorithms and simulated annealing [4, 6, 8] mainly due to their ability to avoid trapping into local optimum of the objective function. In our system we have applied a C++ library of genetic algorithm components (GAlib) developed at the M.I.T. [7] and the adaptive simulated annealing (ASA) given as a C code in [9].

The basic structure of our magnetic field tomography system is shown in Fig. 4.

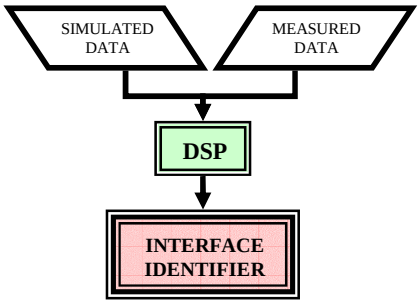

Fig. 4. *Flowchart of the interface shape reconstruction system.*

It consists of two main modules: DSP and Interface Identifier. In the digital signal processing block, it is performed a noise reduction of recorded/simulated signals, a finding of the maximum amplitude time moment and also the spatial fast Fourier analysis of the signals. The spatial FFT enables to shrink the source space of identification i.e. to reduce the number of searching modes existing in the interface shape definition, which could be later used in the Interface Identifier (Fig. 5).

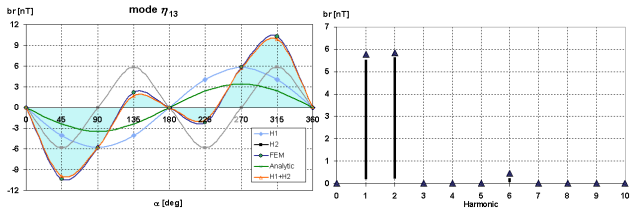

Fig. 5. *Radial magnetic field component distribution at z=50 mm and r=35 mm with the spatial harmonic spectrum.*

The DSP block contains also a function based on a measure of correlation between the spatial harmonic spectrum of measured/simulated signals and spectrums stored in the data basis which enables to perform a preliminary estimation of dominant modes and the amplitude of the interface shape.

In the Interface Identifier there are implemented a several versions of genetic algorithms, e.g. simple, steady-state, and incremental in which non-overlapping and overlapping populations are supported, respectively, and additionally the adaptive simulated annealing code adjusted to our problem. In all implemented methods a cost function is calculated with a help of a 3D FEM method which has to be applied to solve the forward problem due to complicated interface shape. Because the number of calculations of the cost function is usually very high the used FEM procedure has to be very effective to reduce the time of calculations. In the next section we show some results received from the reconstructions performed on the simulated data.

3. SAMPLE RESULTS OF RECONSTRUCTIONS

As the first example we present the reconstruction of the mode η_{13} using signals with 20% white noise from the 8 radial sensors located in the middle of the cylinder. Fig. 6 shows the configuration setup of our simulations and the original interface shape of the mode η_{13} together with the FEM mesh used in the forward calculations. In Fig. 7, the distribution of the radial magnetic flux component around the cylinder and the orientation angles related to the interface shape are presented. The cost function (*CF*) in these simulations has been defined as:

$$CF = \sqrt{\sum_{i=1}^{N} \left(b'_{ri} - b_{ri} \right)^2}, \qquad (1)$$

where N is the number of sensors, b'_r and b_r are radial components at sensor positions of actually calculated and reference magnetic field respectively. Additionally we have defined the measure of interface reconstruction quality $\Delta\eta^*$:

$$\Delta\eta^* = \frac{\sqrt{\frac{1}{N}\sum_{i=1}^{N}\left(z_i^{'} - z_i\right)^2}}{A}\cdot 100\,\% \qquad (2)$$

where N is the number of sample points on the interface, z_i is the z-coordinate of the sample point, and A is the amplitude of the original interface.

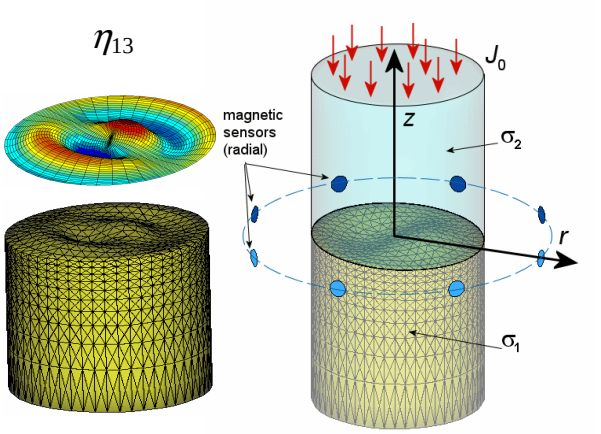

Fig. 6. *Two-fluid cell with 8-radial-sensor-ring with FEM model and the interface shape of mode* η_{13}

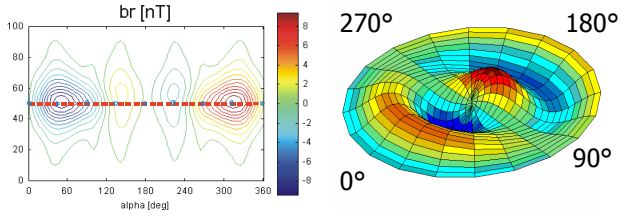

Fig. 7. *Distribution of* b_r *component around cylinder at the radius* r=35 *mm (position of sensor ring is marked with dashed line).*

We have performed several reconstructions using Interface Identifier with the genetic algorithm function for different types of genomes i.e. binary, binary with gray coding, and real representation. We have applied two versions of genetic algorithm: simple and modified with multi-loop scaling [4]. Fig. 8 shows the results of reconstructions together with the values of quality of the interface reconstruction. The best reconstruction result has been received for the multi-loop simple genetic algorithm with gray coded binary genome representation. Fig. 9 presents the quality of interface reconstruction versus values of the best found cost function. We can observe a main concentration of points for small cost function values. This means that it is very difficult to distinguish various interface shapes using only the signals from 8 sensors.

Following above remark we have performed the next simulations in which we have increased the number of sensors. Despite of the previous sensors located in the middle of cylinder, we have used additionally 8 sensors moved in z direction of 15 mm (Fig. 10). In that position we can also measure the z component of the magnetic field, so the cost function for these simulations takes the following form:

$$CF = \sqrt{\sum_{i=1}^{N}\left(b_{ri}^{'} - b_{ri}\right)^2 + \left(b_{zi}^{'} - b_{zi}\right)^2}\,. \qquad (3)$$

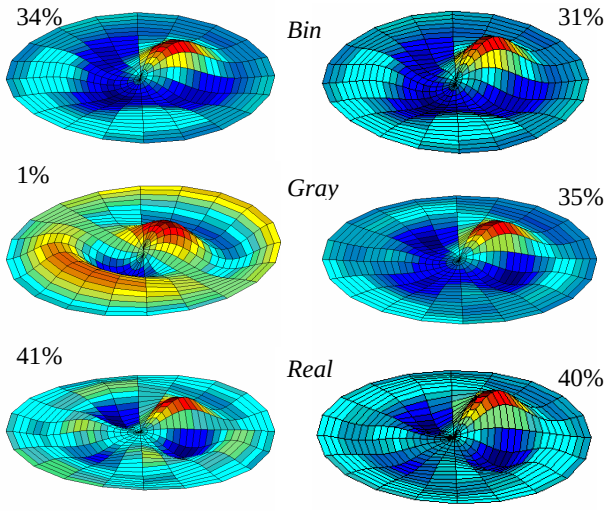

Fig. 8. *Results of reconstruction of mode* η_{13} *with simple GA (right) and multi-loop GA (left) for different coding and genomes (one sensor ring configuration).*

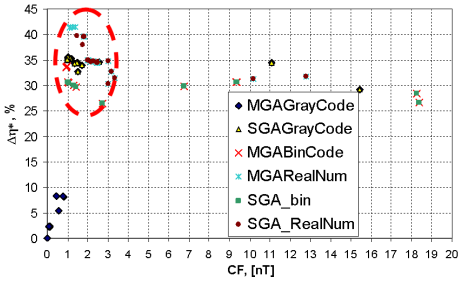

Fig. 9. *Quality of the interface reconstruction versus cost function values for different versions of genetic algorithm.*

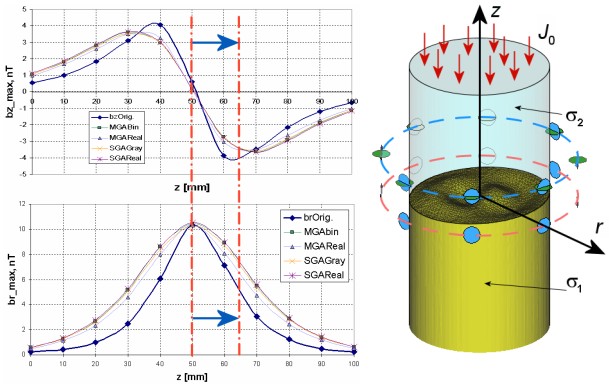

Fig. 10. *Configuration with two rings (*b_r *and* b_z *sensors) and the distribution of magnetic flux density at sensor positions.*

Fig 11 shows the distribution of radial and *z*-component around the cylinder with the marked sensor positions.

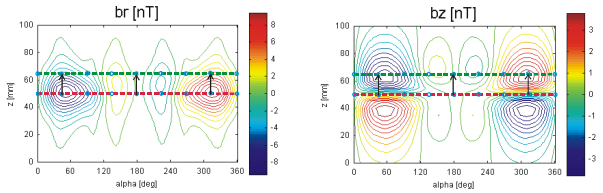

Fig. 11. *Distribution of b_r and b_z components around cylinder at the radius r=35 mm (positions of sensor rings are marked with dashed lines).*

The results presented in Fig. 12 shows that the quality of reconstructions in these simulations was in every case better. The spread of concentration of quality versus *CF* points is also better in that case.

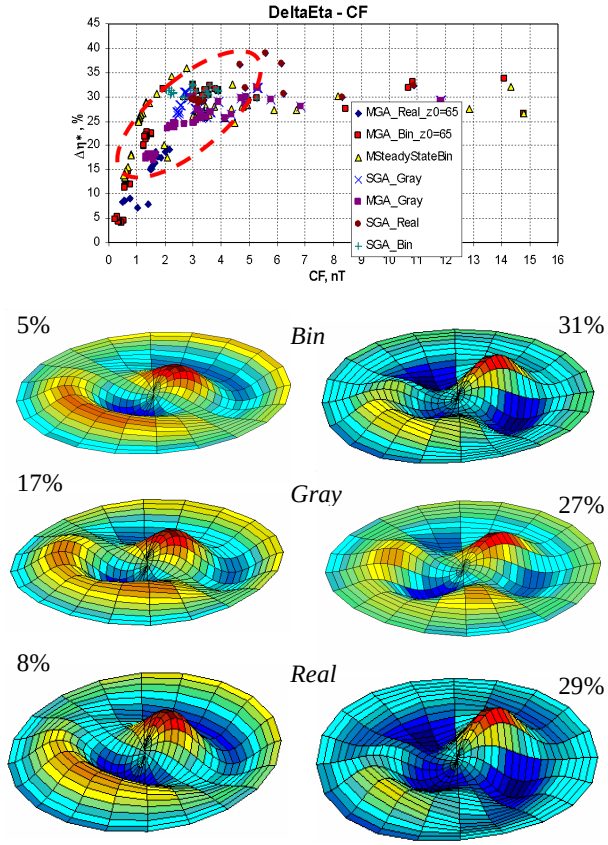

Fig. 12. *Quality of interface reconstruction versus cost function values (above) and results of reconstruction of mode η_{13} with simple GA (right) and multi-loop GA (left) for different coding and genomes (two sensor rings configuration).*

3. CONCLUSIONS

Interface shape between the two conducting fluids is identified with sufficient accuracy with our magnetic field tomography system for simulated magnetic. Accuracy of reconstruction depends strongly on the number and positions of sensor points. The common genetic optimization is enough sensitive for solving the magnetic fluid dynamics inverse field problem but is much too slowly. The efficiency of the optimization process can be improved by applying the DSP module to reduce the GA source search space. Further experiments with measured data are currently into investigation.

REFERENCES

[1] P.A.Davidson, "Magnetohydrodynamics in material processing," *Annu. Rev. Fluid Mech.*, vol. 31, pp. 273-300, 1999

[2] J. Miles, and D. Henderson, "Parametrically forced surface waves," *Annu. Rev. Fluid Mech.,*vol. 22, pp. 143-165, 1990.

[3] H. Brauer, M. Ziolkowski, M.Kuilekov, "A Magnetic Field Tomography System for Interface Reconstruction in Magnetic Fluid Dynamics," *this conference*.

[4] M. Ziolkowski, H. Brauer, M. Kuilekov, "Interface reconstruction between two conducting fluids applying genetic algorithms", *IEEE Transaction on Magnetics*, Vol 40, No 3, 2004 (in press)

[5] S. Men, C. Resagk, M. Ziolkowski, M. Kuilekov, H. Brauer, "Measurement of magnetic flux on a rotating distorted electrolyte-metal interface", *Measurement Science & Technology*, 2004 (accepted)

[6] Z. Michalewicz, *Genetic Algorithms + Data Structures = Evolution Programs*, 3rd ed., Springer Verlag, Berlin, Heidelberg, New York, 1996.

[7] M. Wall, "GAlib: A C++ Library of Genetic Algorithm Components". V2.4, 1996, http://lancet.mit.edu/ga/

[8] L. Ingber, *"Simulated annealing: Practice versus theory"*. Math. Comput. Modelling, vol. 18, No. 11, 1993, pp. 29-57

[9] L. Ingber, *"Adaptive Simulated Annealing (ASA)"*. ASA-User Manual, 2003, http://www.ingber.com/